Equilibrium charge-state distributions of 35—146-MeV Cu ions behind carbon foils

K. Shima, T. Ishihara, T. Miyoshi, and T. Mikumo
Tandem Accelerator Center, University of Tsukuba, Ibaraki 305, Japan
(Received 17 January 1983)

Equilibrium charge-state distributions of Cu ions behind carbon foils have been measured in the energy region 35—146 MeV. The equilibration is obtained with about 30- and 50-$\mu g/cm^2$-thick carbon at energies of 65 and 120 MeV, respectively. Almost-constant values of distribution width have been observed in the 35—47-MeV and 96—146-MeV energy regions. The former corresponds to the Cu ions whose outermost electrons are mainly distributed in the M shell, while the latter in the L shell. The asymmetry of the charge distribution has been observed in the boundary charge state between the Cu L and M shells. Such an asymmetric distribution function has been well approximated with the connection of two Gaussian distributions with an equal centroid but with different standard deviations.

I. INTRODUCTION

All the charge-state distribution data of energetic ions for Z_1 (projectile atomic number) >2 before 1972 are summarized in the compilation of Wittkower and Betz.[1] In that compilation, the data of fast heavy ions ($Z_1>10$ and energy $E>10$ MeV) are scarce and are limited to the ions of S ($E<52$ MeV), Cl ($E<40$ MeV), Br ($E<140$ MeV), Kr ($E<505$ MeV), I ($E<160$ MeV), Ta ($E<148$ MeV), and U ($E<150$ MeV). Since 1972, measurements for such fast heavy ions have been reported by Deschepper *et al.* for 72—123-MeV P ions,[2] by Scharfer *et al.* for 69—142-MeV S ions,[3] by Ishihara *et al.* for 25—140-MeV Si and Cl ions,[4] by Knystautus *et al.* for 3—20-MeV Ar ions,[5] by Clark *et al.* for various heavy ions,[6] by Baron *et al.* for 373—552-MeV Kr ions,[7] and by Moak *et al.* for 20-MeV I ions.[8] As a result, equilibrium mean charge states of heavy ions behind the solid target have been precisely investigated over the wide energy region[9,10] and Z_1 as well as Z_2 (target atomic number) dependence of the charge states have been partially clarified.[3,7,9,11—13]

On the other hand, as for the charge distribution width and the charge distribution function, the recognition is still poor. Current empirical formulas for the distribution width by Nikolaev and Dmitriev[14] or by Betz and Schmelzer[15] are reported to deviate significantly from the observed 3—20-MeV Ar ion data.[5] Baudinet-Robinet approximated the distribution function with χ^2, Gaussian and reduced χ^2 distributions for low, intermediate, and high ionic velocity regions, respectively.[16,17] However, the asymmetric charge distributions of Br or I ions reported by Datz *et al.*[18] at intermediate-velocity regions, are far from the simple Gaussian shape. Since the shell effect is involved, the analysis of the charge states for such rather heavy ions becomes complicated compared with the analysis for relatively light heavy ions. To obtain a comprehensive understanding, more data for such rather heavy ions are needed.

In this work, the equilibrium charge-state distributions of Cu ions after emergence from carbon foil have been measured for Cu energies of 35—146 MeV. In this energy region, projectile velocities range from $4.7v_0$ to $9.7v_0$, where v_0 means the Bohr velocity. On the other hand, the mean velocity of the projectile L-shell electrons is about $9v_0$ and that of the M-shell electrons for partially ionized Cu ions is about $3v_0$. Therefore, depending on the projectile energy, the appeareance of some shell effect which is characteristic to the projectile L and M shells is expected with respect to the charge distribution function and the distribution width. Many authors point out the rapid change of the adjacent charge fraction ratios at the boundary charge state between the K and L shells. Although such shell effects were first observed in the L-M—shell boundary charge state by Moak *et al.*,[19] no systematic observation of the distribution width or numerical analysis for the asymmetric distribution function has been done taking into account the shell effect. It is the purpose of this paper, firstly, to present the charge distribution data of Cu ions and, secondly, to find some relationship between the charge distribution function and the distribution width in conjunction with the effect of the projectile shell structure.

II. EXPERIMENTAL

The detail of the experiment for the charge distribution measurement at the University of Tsukuba is given elsewhere.[4] The ^{63}Cu ion beam (2 mm in diameter) supplied by the tandem accelerator passed through a carbon foil. The projectile charges behind the foil were analyzed with a magnetic spectrograph (Enge split-pole type 90) and the beam current for the charge state q was collected with a Faraday cup which was led to a beam current integrator. Elastically scattered Cu ions were detected with a surface barrier semiconductor detector whose counts during the run served as a monitor for the determination of the charge-state fraction $F(q)$.

Observed charge distribution data are to be analyzed with respect to the projectile exit energy from the foil. For that purpose, exit energies have been estimated

through two different methods. One is to estimate the projectile energy loss which is the product of stopping power[20] and carbon foil thickness measured with the use of ^{241}Am-α particles. The other method is to estimate the exit energy from the difference of the magnetic fields (operated to analyze the charge states) between the cases with and without the carbon foil. The exit energies thus obtained with two methods agree within the error of 0.25 MeV.

III. RESULT

Before measuring the equilibrium charge distribution, nonequilibrium charge distribution was measured for fixed incident energies of 65 and 120 MeV. In Fig. 1, the charge-state fraction $F(q)$ and the mean charge state $\bar{q}$ are plotted as a function of carbon foil thickness for the incidence of 65-MeV Cu^{9+} ions. Here, the mean charge state $\bar{q}$ is defined as

$$\bar{q}=\sum_q qF(q) . \tag{1}$$

The figure indicates that the equilibration is attained at the foil thickness greater than about 30 μg/cm^2. At this projectile energy, with the mean charge state being about $\bar{q}=18$, the fractions of charge states $q>18$ are seen to decrease with increasing foil thickness corresponding to the decrease of the exit energy. With the increase of foil thickness, the mean charge states similarly show the decreasing behavior after the equilibration is attained. As is seen later (Figs. 2 and 3), when $F(q)$ or $\bar{q}$ values are plotted as a function of exit energy, those values, if the equilibration is attained, are smoothly linked up with each other even if the incident energy is fixed. In the case of the 120-MeV Cu^{11+} incidence, equilibration has been observed to reach about 50-μg/cm^2-thick carbon foil. Considering the above thicknesses for the attainment of equilibration, foil thicknesses were properly selected for the measurement of equilibrium charge states.

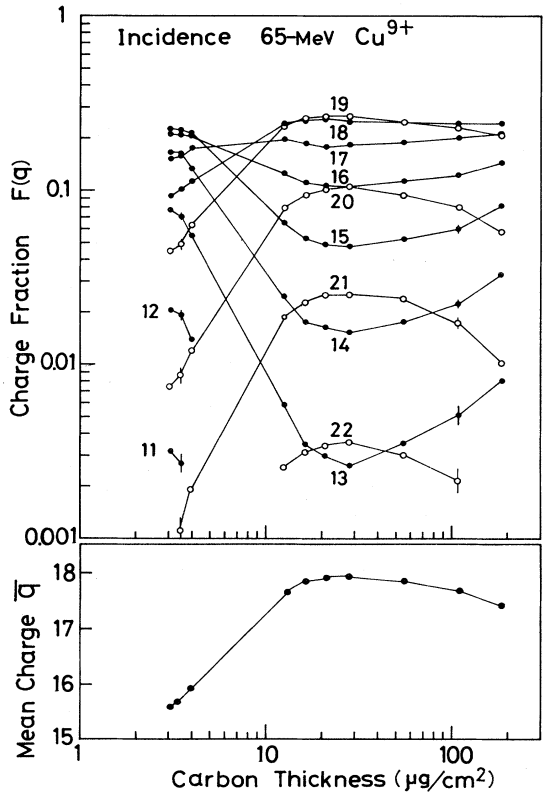

FIG. 1. Charge fractions $F(q)$ (upper) and mean charge states $\bar{q}$ (lower) for 65-MeV Cu^{9+} incident ions in carbon foils between 3.1 and 183 μg/cm^2. Curves are drawn to guide the eye.

In Table I, the result of equilibrium charge-state fractions $F(q)$ are listed together with the $\bar{q}$ values and the distribution width d which is defined as

$$d=\left[\sum_q (q-\bar{q})^2F(q)\right]^{0.5} . \tag{2}$$

In the table, projectile incident energy, exit energy, and carbon foil thickness are also listed. Errors come from the uncertainties in the beam current integration and the statistics of the monitor detector counts. Judging from the reproducibility of the measurement, the maximum errors are estimated to be less than 2.5% for $F(q)>0.08$, 8% for $F(q)>0.01$, and 18% for $F(q)<0.01$.

In Fig. 2, $F(q)$ values are plotted as a function of exit energy. It should be noted that the rapid increase of the envelope connecting the maxima of the fractions takes place in between the charge-state group of $q\leq 18$ and $q\leq 19$. This is one of the characteristics provided by the shell effect. As is clarified in Sec. IV, this phenomenon corresponds to the fact that the distribution width of the charge-state group $q\geq 19$ is narrower than that of the group $q\leq 18$. Similar trend is seen in the charge distributions of Ar ions behind carbon foils[5] where the rapid change of the envelope takes place between the maximum charge fractions of $q=7$ and 8.

IV. DISCUSSION

A. Mean charge state

Mean charge states $\bar{q}$ divided by Z_1 for Cu ions are shown in Fig. 3 as a function of reduced velocity X defined by

$$X=v/(3.6\times 10^8 Z_1^{0.45}) , \tag{3}$$

where v is the ion velocity in cm/sec. This reduced velocity was first introduced by Nikolaev and Dmitriev[14] and is known to be a good parameter for the scaling procedure of equilibrium charge states in ion-solid collisions. In the figure are also drawn the $\bar{q}$ values of Cl and Br ions observed behind carbon foils by Ishihara *et al.*[4] and Datz *et al.*[18], respectively, and empirical formulas by Nikolaev and Dmitriev,[14]

$$\bar{q}/Z_1=(1+X^{-1/0.6})^{-0.6} , \tag{4}$$

and by Shima *et al.*[9],

$$\bar{q}/Z_1=1-\exp(-1.25X+0.32X^2-0.11X^3) . \tag{5}$$

TABLE I. Mean charge state $\bar{q}$, width of charge distribution d, and equilibrium charge-state fraction $F(q)$ of Cu ions after passage through carbon foils.

Incident energy (MeV)	Exit energy (MeV)	Carbon thickness (μg/cm^2)	Mean charge $\bar{q}$	Distribution width d	Charge Fraction $F(q)$ (%)				
					11+	12+	13+	14+	15+
150	146.4	112	21.66	1.35					
135	130.9	109	21.17	1.32					
120	117.1	55	20.68	1.32					
120	115.8	109	20.62	1.34					
120	112.9	183	20.46	1.34					
100	95.6	109	19.79	1.33					
80	75.5	109	18.76	1.40					1.57
65	62.7	55	17.86	1.53			0.35	1.78	5.26
65	60.4	109	17.72	1.55			0.52	2.21	6.05
65	57.3	183	17.43	1.57			0.82	3.31	8.24
50	46.9	74	16.46	1.65		0.71	3.28	8.51	15.7
50	43.3	183	15.93	1.66		1.69	5.80	12.8	19.7
43	40.7	55	15.79	1.68	0.35	2.15	6.48	14.1	19.8
43	35.5	183	15.11	1.64	0.92	4.22	11.6	19.5	23.2

Although it is reported[9] that the better fitting is obtainable with Eq. (5) for the heavy-ion data of the high-velocity region ($X > 1.5$), there seems to be little difference between Eqs. (4) and (5) in the velocity region drawn in the figure. Present Cu ion data as well as other heavy-ion data are seen to be reproduced by either Eq. (4) or (5) within the uncertainty of $\Delta q/Z_1 = 0.03$.

B. Distribution width

The distribution width defined by Eq. (2) corresponds to the standard deviation in the case of a Gaussian distribution. In Fig. 4(a) observed distribution widths are shown as a function of the Cu exit energy. The mean charge states taken from Fig. 3 are indicated at the top of the figure. The empirical formulas for the width by Betz and Schmelzer,[15]

$$d = 0.27 Z_1^{0.5} , \tag{6}$$

and by Nikolaev and Dmitriev,[14]

$$d = 0.5 Z_1^{0.5} (1 + X^{-1/0.6})^{-0.8} X^{-1/1.2} , \tag{7}$$

are also drawn. Equations (6) and (7) were obtained empirically based on some experimental data. For the deduction of Eq. (7), Gaussian distribution was assumed for the charge distribution and Bohr criterion was used.[14,21] Experimental points are seen to deviate significantly from Eqs. (6) and (7) with respect to the magnitude and the energy dependence.

Figure 4(a) shows that the distribution widths exhibit an almost plateau feature both in the lower ($35 < E < 50$ MeV) and higher ($90 < E < 150$ MeV) energy regions tested at the present time. Judging from the mean charge values which vary from about $\bar{q} = 15$ to $\bar{q} = 22$, the outermost electrons, the fractions of which contribute dominantly to the width value, are distributed among the M shell in the lower energy plateau, while at the higher energy plateau outermost electrons are mainly distributed among L shell. This fact means that the electrons, so far as they are included within a certain shell, are statistically distributed with the width remaining constant, although the centroid of the distribution varies as a function of projectile energy. It further indicates that the distribution width differs according to which shell the outermost electrons are mainly distributed among. Probably the factor which determines the magnitude of the width is in the number of electrons to be occupied in the shell or subshell.

If we combine the Cu data with the widths of Si, Cl, and Ar ions observed behind carbon foils by others,[4,5,22–25] the dependence of the distribution width on the outermost shell electrons becomes clearer. In Fig. 4(b) the relation $d/Z_1^{0.26}$ versus reduced velocity X is shown. The ordinate scale is properly taken so that the widths of the plateau region due to the distribution of L-shell electrons come together. For Cl, Ar, and Cu ions, the distribution width is seen to vary from the higher plateau value (dominated by the M-shell electron distribution) to the lower plateau value (dominated by the L-shell electron distribution). In the high-velocity region of $X > 1.5$, where the distribution of K-shell electrons affects the width, the distribution width decreases with increasing projectile velocity as is seen in the cases of Si and Cl ions.

C. Charge distribution function

According to Baudinet-Robinet,[16,17] the charge distribution function is approximated by the reduced χ^2 distribution at the high-velocity region where the mean charge states come close to Z_1 and is approximated with the Gaussian distribution in the intermediate-velocity region. However, the asymmetric distributions of rather heavy ions such as Br or I reported by Datz *et al.*[18] are far from the Gaussian or χ^2 distribution. This is because the shell

TABLE I. (*Continued.*)

Charge Fraction $F(q)$ (%)									
16 +	17 +	18 +	19 +	20 +	21 +	22 +	23 +	24 +	25 +
		0.68	4.77	14.6	24.7	27.9	19.1	7.09	1.04
		1.60	8.82	20.5	29.1	24.4	12.1	3.19	0.34
	0.75	3.30	14.9	25.7	28.7	18.3	6.90	1.40	
	0.82	3.81	15.5	26.7	28.0	17.4	6.45	1.24	0.09
0.20	1.15	4.65	17.5	27.9	27.2	15.3	5.23	0.91	
0.93	3.48	10.1	27.0	29.6	19.5	7.46	1.68	0.19	
4.78	11.1	21.0	32.6	19.8	7.43	1.63	0.18		
11.3	18.9	24.9	25.7	9.32	2.39	0.30			
12.2	20.1	24.9	24.0	8.07	1.73	0.22			
14.6	21.1	24.4	20.7	5.76	1.02				
21.5	21.9	17.2	9.55	1.50	0.16				
22.2	19.5	12.4	5.38	0.63					
22.4	18.6	11.2	4.49	0.46					
20.1	13.0	5.76	1.67						

effect is involved in the electron-capture and -loss processes and the behavior of the projectile electrons is characterized according to which shell the electron belongs. In fact, when the ratios of adjacent charge fractions $F(q+1)/F(q)$ of the present Cu data are plotted in Fig. 5 as a function of charge state q, the change of the slope is seen to take place at the boundary charge state between the L shell and the M shell. If we notice that (1) the slope of $F(q+1)/F(q)$ differs according to the groups of $q \geq 19$ or $q \leq 18$, but is nearly independent of the projectile energy, and if we consider the previously obtained information that (2) the distribution width is almost constant for ions whose outermost electrons are mainly distributed either in the L shell or the M shell, then, the charge distribution function for Cu ions is considered to be composed of two Gaussian distributions with an equal centroid, but with different standard deviations d_L and d_M. The function may be expressed as

$$F(q)_L = \frac{A_L}{\sqrt{2\pi}d_L} \exp[-(q-\bar{q})^2/(2d_L^2)] \quad \text{for } q \geq 19 \tag{8}$$

$$F(q)_M = \frac{A_M}{\sqrt{2\pi}d_M} \exp[-(q-\bar{q})^2/(2d_M^2)] \quad \text{for } q \leq 18$$

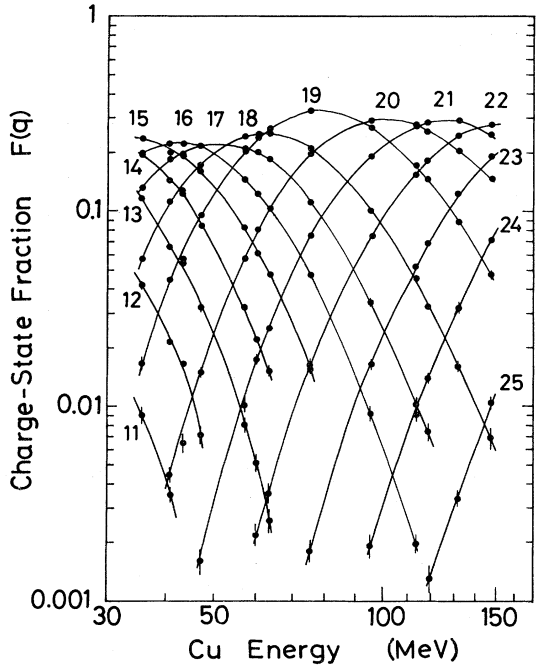

FIG. 2. Equilibrium charge fractions of Cu ions after passage through carbon foils as a function of Cu energy of emergence from the foil. Curves are drawn to guide the eye.

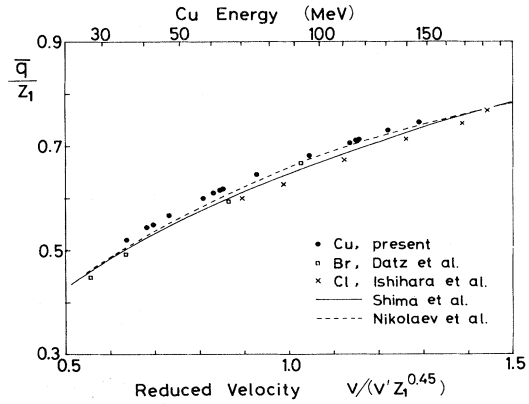

FIG. 3. Mean charge states $\bar{q}$ divided by Z_1 vs reduced velocity $v/(v'Z_1^{0.45})$, where $v'=3.6\times10^8$ cm/sec. In addition to the data of Cu ions (present), Br ions (Datz *et al.*) and Cl ions (Ishihara *et al.*), observed behind the carbon foil, the empirical relations by Shima *et al.* and by Nikolaev *et al.* are drawn.

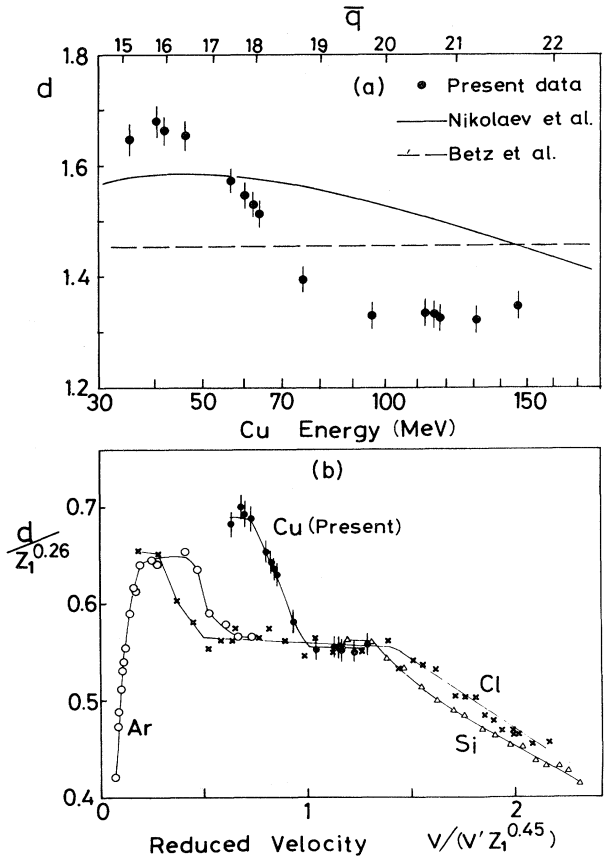

FIG. 4. Distribution widths. (a) Observed widths for Cu ions and the relations for the width by Nikolaev *et al.* and by Betz *et al.* are shown as a function of the projectile exit energy from the foil. (b) Distribution widths divided by $Z_1^{0.26}$ for Cu, Ar, Cl, and Si ions behind carbon foils are plotted as a function of reduced velocity. Data of Ar, Cl, and Si ions are taken from Refs. 4, 5, 16, 17, 18, and 19. Solid lines are drawn to guide the eye.

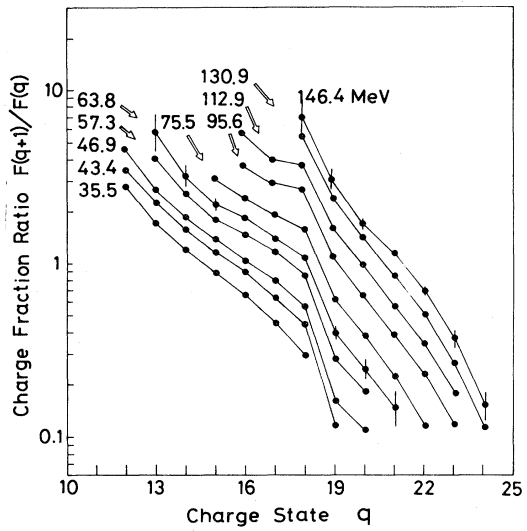

FIG. 5. Charge fraction ratios $F(q+1)/F(q)$ for various energies of Cu ions after emergence from the carbon foils are shown as a function of the charge state q.

where A_L and A_M are normalization factors connected with

$$\sum_{q\geq 19} F(q)_L + \sum_{q\leq 18} F(q)_M = 1 \ . \tag{9}$$

From the distribution widths in Fig. 4(a), it is reasonable to take the constant d_L and d_M values as $d_L = 1.34$ and $d_M = 1.66$. In Fig. 6 observed charge distributions of 95.6-, 75.5-, and 46.9-MeV Cu ions are shown as a function of charge state q. Two Gaussian distributions fitted with Eq. (8) are drawn with solid lines. The A_L and A_M values adopted for the best fitting to the observed data are described in the figure. Asymmetric distribution presented by the shell effect is seen to be well approximated with the connection of two Gaussian distributions. It should further be mentioned that the distribution functions approach the single Gaussian distribution for the cases of $E > 95.6$ MeV or $E < 46.9$ MeV, in which the charge fractions are mostly composed of charge states $q \geq 19$ or $q \leq 18$.

Instead of the present procedure to connect two Gaussian distributions, Sayer[10] introduced an asymmetric parameter ϵ, and adopted the following modified Gaussian distribution for the expression of the asymmetric charge distribution:

$$F(q) = F_m \exp[-0.5t^2/(1+\epsilon t)] \ , \tag{10}$$

where $t = (q - q_0)/\rho$ and F_m indicates the maximum charge fraction for the maximum charge state q_0. It was shown that the observed asymmetric distribution data were better fitted with Eq. (10) than with the Gaussian distribution. In Eq. (10) the concept of shell effect is not included. Instead, the best fitted values of ϵ or ρ for many asymmetric distribution data should automatically exhibit the shell characteristic feature if ϵ or ρ values are plotted with some suitable function of Z_1 and v. For that purpose, more asymmetric distribution data are necessary over the wide range of Z_1 and v. For the comprehensive interpretation of shell effect on the distribution function or width, different approaches from different aspects such as Eqs. (8) and (10) should be done.

D. On the BG model

Equilibrium charge states of heavy ions behind the solid target are known to be higher than those behind the gas target. According to Betz and Grodzins[26] (BG model) the difference of these charge states is mainly due to the Auger electron emissions after emergence from the foil, whereas, according to Bohr and Lindhard[27] (BL model), the ionic charges inside the foil are already higher than those in gas. Many authors have discussed this problem[12,28–30] but a final conclusion has not been obtained. In the following, the viewpoint for the case of Cu + C collision is described.

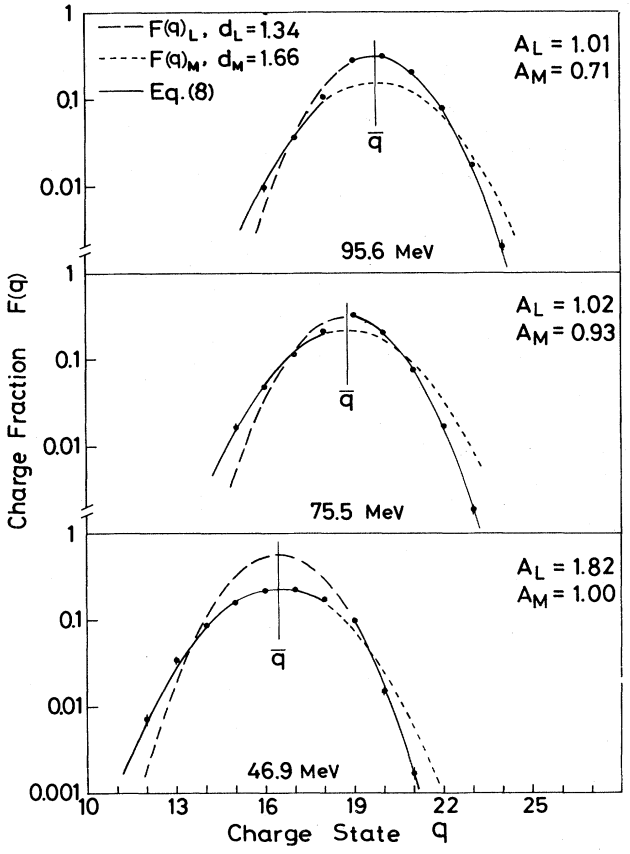

FIG. 6. Charge distribution data of 95.6-, 75.5-, and 46.9-MeV Cu ions. Broken lines $F(q)_L$ and the dotted lines $F(q)_M$ are the Gaussian distributions whose standard deviations are $d_L = 1.34$ and $d_M = 1.66$, respectively. Solid lines are the curves of $F(q)_L$ for $q \geq 19$ and $F(q)_M$ for $q \leq 18$. The centroid of the distribution $q = \bar{q}$ is common to $F(q)_L$ and $F(q)_M$, and is taken from the experimental mean charge state.

For Cu ions, charge distribution data for the gas target are not reported. However, with the aid of the empirical formula for the mean charge state of ions behind the gas target,[31] the $\bar{q}$ (gas) of Cu ions is estimated to be about 3 to 4 charge states lower than the $\bar{q}$ (solid) value over the present Cu ion energy range. Suppose this charge-state difference is mainly due to the post foil deexcitation process as was suggested by the BG model; the ionic charge state inside the foil should then be shifted by about 3 or 4 charge states compared to the observed charge state behind the foil. Within the foil, equilibration is attained on the balance of electron-loss and -capture processes, both of which are strongly dependent on the projectile atomic shell structure. Experimental evidence of $F(q+1)/F(q)$ vs q in Fig. 5 demonstrates that such a shell-dependent characteristic feature, which should originally take place inside the foil, has been observed even behind the solid target without any shift of the charge state from the boundary charge state between Cu L shell and M shell. This fact suggests that the effect of the post foil Auger electron emission is not so strong as to completely shade off the shell effect inside the foil. However, because the shell effect was observed in the $F(q+1)/F(q)$, it does not mean that the post foil Auger effect is of little importance. Shell effect, which is not observed in $\bar{q}$, is visible only when the more sensitive probe [such as $F(q+1)/F(q)$ or d] is used for the inspection of the shell effect. Moreover, Shima *et al.*[32] observed the Cu K x-ray spectrum in 150-MeV Cu + C collision, and estimated the charge state of excited Cu ions inside the foil to be $\bar{q} = 19$ or 20. This value is apparently lower than the $\bar{q}$ value observed behind the foil (see Table I, $\bar{q} = 21.66$ at $E = 146.4$ MeV), which indicates the increase of charge state after emergence from the foil. In order to interpret the evolution of the charge state of projectiles passing through matter, discussion based on the qualitative analysis of projectile charge state is necessary.

V. CONCLUSION

Equilibrium charge-state distribution of 35–146-MeV Cu ions have been measured after the passage through carbon foils. Equilibration is attained for carbon thicknesses greater than about 30 and 50 $\mu g/cm^2$ for Cu energies of 65 and 120 MeV, respectively. $\bar{q}$ values are in good agreement with current empirical formulas. Distribution width plotted as a function of projectile energy has exhibited two plateau regions, i.e., the region with a broader width corresponding to the Cu ions whose outermost electrons are dominantly distributed in Cu M shell, and the region with a narrower width corresponding to the ions in which outermost electrons are mainly distributed in the L shell. The asymmetric charge distribution functions are well approximated with the connection of two Gaussian distributions with different standard deviations but with the value of common centroid. The connection of two Gaussian distributions has been done considering the shell effect which was observed in the boundary charge state between Cu L and Cu M shells.

ACKNOWLEDGMENTS

The assistance of K. Numata, K. Michikawa, and the staff of the tandem accelerator center with the performance of this experiment is gratefully acknowledged. This work was supported in part by the Nuclear and Solid-State Research Project of the University of Tsukuba.

[1]A. B. Wittkower and H. D. Betz, At. Data 5, 113 (1973).
[2]Ph. Deschepper, P. Lebrun, J. Lehmann, L. Palffy, and P. Pellegrin, Nucl. Instrum. Methods 166, 531 (1979).
[3]U. Scharfer, C. Henrichs, J. D. Fox, P. von Brentano, L. Degener, J. C. Sens, and A. Pape, Nucl. Instrum. Methods 146, 573 (1977).
[4]T. Ishihara, K. Shima, T. Kimura, S. Ishii, T. Momoi, H. Yamaguchi, K. Umetani, M. Moriyama, M. Yamanouchi, and T. Mikumo, Nucl. Instrum. Methods 204, 235 (1982).
[5]E. J. Knystautus and M. Jomphe, Phys. Rev. A 23, 679 (1981).

[6]R. B. Clark, I. S. Grant, R. King, D. A. Eastham, and T. Joy, Nucl. Instrum. Methods 133, 17 (1976).
[7]E. Baron and B. Delaunay, Phys. Rev. A 12, 40 (1975).
[8]C. D. Moak, L. B. Bridwell, H. A. Scott, G. D. Alton, C. M. Jones, P. D. Miller, R. O. Sayer, Q. C. Kessel, and A. Antar, Nucl. Instrum. Methods 150, 529 (1978).
[9]K. Shima, T. Ishihara, and T. Mikumo, Nucl. Instrum. Methods 200, 605 (1982).
[10]R. O. Sayer, Rev. Phys. Appl. 12, 1543 (1977).
[11]W. N. Lennard and D. Phillips, Phys. Rev. Lett. 45, 176 (1980).
[12]W. N. Lennard, T. E. Jackman, and D. Phillips, Phys. Rev. A 24, 2809 (1981).
[13]K. Shima, T. Ishihara, T. Momoi, T. Miyoshi, K. Numata, and T. Mikumo, Phys. Lett. A (in press).
[14]V. S. Nikolaev and I. S. Dmitriev, Phys. Lett. 28A, 277 (1968).
[15]H. D. Betz and Ch. Schmelzer, Unilac Report No. 1-67, Universität Heidelberg, 1967 (unpublished).
[16]Y. Baudinet-Robinet, Nucl. Instrum. Methods 190, 197 (1981).
[17]Y. Baudinet-Robinet, Phys. Rev. A 26, 62 (1982).
[18]S. Datz, C. D. Moak, H. O. Lutz, L. C. Northcliffe, and L. B. Bridwell, At. Data 2, 273 (1971).
[19]C. D. Moak, H. O. Lutz, L. B. Bridwell, L. C. Northcliffe, and S. Datz, Phys. Rev. Lett. 18, 41 (1967).
[20]L. C. Northcliffe and R. F. Schilling, Nucl. Data Tables A7, 233 (1970).
[21]I. S. Dmitriev and V. S. Nikolaev, Zh. Eksp. Teor. Fiz. 47, 615 (1964). [Sov. Phys.—JETP 20, 409 (1965)].
[22]E. Almqvist, C. Broude, M. A. Clark, J. A. Kuehner, and A. E. Litherland, Can. J. Phys. 40, 954 (1962).
[23]A. B. Wittkower and G. Ryding, Phys. Rev. A 4, 226 (1971).
[24]P. Hvelplund, E. Laegsgard, J. O. Olsen, and E. H. Pedersen, Nucl. Instrum. Methods 90, 315 (1970).
[25]P. L. Smith and W. Whaling, Phys. Rev. 188, 36 (1969).
[26]H. D. Betz and L. Grodzins, Phys. Rev. Lett. 25, 211 (1970).
[27]N. Bohr and J. Lindhard, K. Dan. Vidensk, Selsk. Mat.-Fys. Medd. 28, no. 7 (1954).
[28]C. D. Moak, IEEE Trans. Nucl. Sci. NS-23, 1126 (1976).
[29]H. Geissel, Y. Laichter, W. F. W. Schneider, and P. Armbruster, Nucl. Instrum. Methods 194, 21 (1982).
[30]R. A. Baragiola, P. Ziem, and N. Stolterfoht, J. Phys. B 9, L449 (1975).
[31]H. D. Betz, Rev. Mod. Phys. 44, 465 (1972).
[32]K. Shima, K. Umetani, T. Mikumo, H. Kano, Y. Tagishi, M. Yamanouchi, Y. Iguchi, and H. Yamaguchi, in *Inner-Shell and X-Ray Physics of Atoms and Solids,* edited by D. J. Fabian, H. Kleinpoppen, and L. M. Watson, (Plenum, New York, 1981), p. 189.